

Finite velocity meson exchange in nuclei

Michael A. Crecca and G. E. Walker

Indiana University Nuclear Theory Center, 2401 Milo B. Sampson Lane, Bloomington, Indiana 47405

(Received 5 October 1990)

Many-body techniques are used to develop a practical formalism for including an energy-transfer dependence in the nucleon-nucleon interaction used in nuclear linear response models. An energy-transfer dependence is naturally expected from the exchange of finite mass, finite velocity mesons. The formalism is applied in a Tamm-Dancoff approximation model structure calculation for ^{16}O . The importance of meson retardation effects on the structure calculation is studied as a function of the magnitude of unperturbed particle-hole energies. The relative importance of ring and ladder contributions is also investigated. It is found that retardation effects can become qualitatively important when particle-hole energies are comparable to the mass of the exchanged meson as would be the case for N^* particle-nucleon hole configurations. While ladder kernels exhibit a significant energy-transfer dependence, the actual results obtained including retardation when solving for the ladder polarization propagator follow closely the results obtained using an instantaneous ladder kernel. This result suggests a simple procedure for including retardation effects.

I. INTRODUCTION

Historically, most effective nucleon-nucleon interactions used in nuclear structure or reaction studies have either been of the type that contain no dependence on the relative time between virtual meson emission and absorption [e.g., $V \equiv V(\mathbf{x}, \mathbf{x}')$] or interactions containing a delta function in the relative time [e.g., $V \equiv V(\mathbf{x}, \mathbf{x}')\delta(t - t')$]. The Fourier transform of the former interaction allows for no energy transfer while the latter is independent of the energy transfer. One expects an energy-transfer dependence associated with virtual meson exchange that would be similar to that characteristic of the Klein-Gordon propagator, i.e.,

$$(\mathbf{q}^2 - \omega^2 + m_B^2 - i\epsilon)^{-1},$$

where m_B is the mass of the meson exchanged. Previously it has been shown¹ that, for nuclear matter comprised of nonrelativistic nucleons coupled to vector and scalar mesons in one-space and one-time dimension, dynamic mesons produce small changes in observables compared to a static potential theory. Apparently systematic studies in three-space dimensions and one-time dimension for finite nuclei have not been performed. The purpose of the present investigation is to outline a formalism that can be used to study quantitatively the effects of retarded or finite velocity exchanges on nuclear structure and reaction predictions in three-space and one-time dimensions for finite nuclei. Such a formalism should be of use in studying reactions involving large energy transfer and should naturally be embedded in applications of Dirac phenomenology or relativistic field theory studies in nuclear physics.²

Nonrelativistic or static models typically suppress the energy-transfer term ω in the boson propagator. From examination of the propagator one would expect that retardation effects might not be of qualitative importance

until $\omega \approx m_B$. Thus, for example, studies of low-lying particle-hole excitations (≤ 20 MeV) in the random-phase (RPA) or Tamm-Dancoff approximations (TDA) that have relied on instantaneous interactions [$V \propto \delta(t - t')$] are motivated by the fact that the meson energy transfers expected to be of relevance (~ 20 MeV) are far below the mass of the lightest exchanged meson ($m_\pi \sim 140$ MeV). But to our knowledge the effect of retardation on such low-lying nuclear structure studies has not been investigated quantitatively. The effect on energy-level spectra and the nuclear linear response to external probes (such as the electron) should be investigated as a function of the unperturbed particle-hole energies of the nuclear excitations of interest. It may prove to be necessary to include retardation effects when nucleon internal excitation (isobar particle-nucleon-hole state) plays an important role in the nuclear linear response. In the next section, we use standard many-body techniques to develop the desired formal equations for studying particle-hole excitations including retarded interactions. The equations obtained reduce to the usual RPA and TDA equations in the limit of an instantaneous interaction. In Sec. III we introduce a simple model Lagrangian and truncated space in which to apply the formalism summarized in Sec. II. The model problem allows one to study the effects of retardation in a TDA calculation leading to nuclear spectra and the longitudinal electron-scattering response function in ^{16}O . The strength of the assumed meson-nucleon coupling and mass of the exchanged boson are taken to be consistent with a typical phenomenological instantaneous interaction. The magnitude of the unperturbed particle-hole energies are varied so that the characteristic differences between retarded and instantaneous results can be studied as a function of the unperturbed energy spectrum versus the mass of the boson exchanged. Such a study allows one to estimate more precisely the error involved in ignoring retardation effects in standard low-lying nuclear excitation models as well as suggesting effects that may

be present, for example, in isobar-hole studies of Gamow-Teller strength over a wider excitation energy region. The results obtained in this study are presented and discussed in Sec. IV. Conclusions and suggested further applications are summarized in Sec. V.

II. FORMALISM

The methods of many-body quantum field theory will be employed to calculate the polarization propagator and thus to study the structure of nuclear excitations. In the approach we adopt, the structure of nuclear excitations is characterized by the combination of the nuclear excitation spectrum and "pure" particle-hole excitation admixture coefficients $C_{\beta\alpha}^{(n)}$ associated with the n th excited state. The $C_{\beta\alpha}^{(n)}$ are defined via

$$C_{\beta\alpha}^{(n)} = \langle \Psi_0 | c_{H\alpha}^\dagger(0) c_{H\beta}(0) | \Psi_n \rangle, \quad (2.1)$$

where $|\Psi_0\rangle$ is the full interacting many-body Heisenberg normalized ground state, $|\Psi_n\rangle$ is the n th full interacting many-body normalized Heisenberg state with energy E_n ($H|\Psi_n\rangle = E_n|\Psi_n\rangle$), $c_{H\beta}(0)$ is the Heisenberg representation of the annihilation operator for a single-nucleon state β at time $t=0$, and $c_{H\alpha}^\dagger(0)$ is the Heisenberg representation of the creation operator for a single-nucleon state α at time $t=0$. The random-phase approximation or Tamm-Dancoff approximation which iterate the simplest particle-hole interaction to infinite order, will be used to calculate the polarization propagator.

As a preliminary to discussing the polarization propagator and its relation to nuclear structure, we introduce the following definition of the four-point function $\Pi_{\beta\alpha;\gamma\delta}(y, \mathbf{x}; \mathbf{x}', y')$:

$$i\Pi_{\beta\alpha;\gamma\delta}(y, \mathbf{x}; \mathbf{x}', y') \equiv \langle \Psi_0 | T[\hat{\psi}_{H\alpha}^\dagger(x) \hat{\psi}_{H\beta}(y) \hat{\psi}_{H\gamma}^\dagger(x') \hat{\psi}_{H\delta}(y')] | \Psi_0 \rangle - \langle \Psi_0 | T[\hat{\psi}_{H\beta}(y) \hat{\psi}_{H\alpha}^\dagger(x)] | \Psi_0 \rangle \langle \Psi_0 | T[\hat{\psi}_{H\delta}(y') \hat{\psi}_{H\gamma}^\dagger(x')] | \Psi_0 \rangle, \quad (2.2)$$

where $\hat{\psi}_{H\alpha}(x)$ is the α th component of the fermion field operator $\psi_H(x)$ in the Heisenberg representation

$$\hat{\psi}_H(x) = \sum_{\alpha} \hat{\psi}_{H\alpha}(x) = \sum_{\alpha} \psi_{\alpha}(\mathbf{x}) c_{H\alpha}(t). \quad (2.3)$$

The symbol α denotes a complete set of single-particle state labels.

In diagrammatic language,

$$i\Pi_{\beta\alpha;\gamma\delta}(y, \mathbf{x}; \mathbf{x}', y') = \text{Diagram 1} - \text{Diagram 2}$$

We reduce the four-point function to the usual form³ for the polarization propagator $\Pi_{\beta\alpha;\gamma\delta}(x, x')$ via

$$i\Pi_{\beta\alpha;\gamma\delta}(x, x') = \lim_{\substack{y \rightarrow x^+ \\ y' \rightarrow x'^+}} i\Pi_{\beta\alpha;\gamma\delta}(y, \mathbf{x}; \mathbf{x}', y'). \quad (2.4)$$

The polarization propagator can be expressed in terms of single-particle wave functions, $\psi(\mathbf{x})$, and the polarization propagator Fourier transform in frequency space $i\Pi(\omega)$ as

$$i\Pi_{\beta\alpha;\gamma\delta}(x, x') = \psi_{\beta}(\mathbf{x}) \psi_{\alpha}^*(\mathbf{x}) \psi_{\delta}(\mathbf{x}') \psi_{\gamma}^*(\mathbf{x}') \times \int e^{-i\omega(x^0 - x'^0)} i\bar{\Pi}_{\beta\alpha;\gamma\delta}(\omega) \frac{d\omega}{2\pi} \quad (2.5)$$

(in this paper we use units where $\hbar = c = 1$). The frequency space Fourier transform $i\bar{\Pi}(\omega)$ can be expanded in terms of the admixture coefficients $C_{\beta\alpha}^{(n)}$ and the energy E_n of the n th excited state as³

$$i\bar{\Pi}_{\beta\alpha;\gamma\delta}(\omega) = i \sum_{n \neq 0} \left[\frac{C_{\beta\alpha}^{(n)} C_{\gamma\delta}^{(n)*}}{\omega - (E_n - E_0) + i\eta} - \frac{C_{\alpha\beta}^{(n)*} C_{\delta\gamma}^{(n)}}{\omega + (E_n - E_0) - i\eta} \right]. \quad (2.6)$$

The form of the right-hand side (rhs) of Eq. (2.6) makes it apparent that the poles of $i\bar{\Pi}_{\beta\alpha;\gamma\delta}(\omega)$ occur at the excitation energy $(E_n - E_0)$, and that the residue of $i\bar{\Pi}(\omega)$ at these excitation energies is related to the admixture coefficients $C_{\beta\alpha}^{(n)}$ via

$$\text{Res}[i\bar{\Pi}_{\beta\alpha;\gamma\delta}(\omega = (E_n - E_0))] = C_{\beta\alpha}^{(n)} C_{\gamma\delta}^{(n)*}. \quad (2.7)$$

Thus, a knowledge of the polarization propagator is equivalent to knowing the excitation spectrum and corresponding admixture coefficients.

So far the discussion of the polarization propagator and its relationship to nuclear structure is not limited by assumptions regarding the dynamics or details of the interactions involved. When details of the specific interaction are included, the determination of the polarization propagator is, in general, a difficult task. Our approach to this difficulty is to express, without approximation, the four-point function as a Bethe-Salpeter equation. Then, after making approximations in the Bethe-Salpeter equation, we calculate the polarization propagator. The approximations to the Bethe-Salpeter equation we consider are denoted the RPA and TDA for retarded nucleon-nucleon interactions. We require that they yield the conventional RPA and TDA equations for nuclear structure in the limit of an instantaneous nucleon-nucleon interaction.^{3,4}

As defined, the four-point function consists of all connected diagrams with external legs originating (terminating) at x and x' (y and y') along with the product of two

Bethe-Salpeter inhomogeneity $i\Pi^{(0)}$ as

$$i\Pi_{\beta\alpha;\gamma\delta}^{(0)\text{TDA}}(y,x;x',y') = - \begin{array}{c} \text{Y} \quad \text{X} \\ \beta \downarrow \quad \alpha \downarrow \\ \uparrow \quad \downarrow \\ \gamma \downarrow \quad \delta \downarrow \\ \text{X}' \quad \text{Y}' \end{array} [\theta(\beta-F)\theta(F-\alpha)] \\ = i\Pi_{\beta\alpha;\gamma\delta}^{(0)}(y,x;x',y')\theta(\beta-F)\theta(F-\alpha) \quad (\text{no sum over } \alpha\beta). \quad (2.12)$$

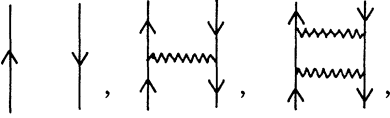
Since the kernels given in (2.10a) and (2.10b) are contained in the full Bethe-Salpeter kernel, and Eq. (2.12) for $\Pi^{(0)\text{TDA}}$ is contained in the full $i\Pi^{(0)}$, the use of K^{TDA} or K^{RDA} in place of K^{BS} along with $i\Pi^{(0)}$ or $i\Pi^{(0)\text{TDA}}$ in the Bethe-Salpeter equation sums, without redundancy, a subclass of diagrams included in (2.8). It is natural to separate the RPA or TDA kernel into ladder and ring parts according to [see Eqs. (2.11c) and (2.11d)]

$$K_{\text{ladder}} = -g^2 D \quad (2.13)$$

and

$$K_{\text{ring}} = g^2 E. \quad (2.14)$$

Repeated application of the ladder kernel alone gives rise to diagrams such as

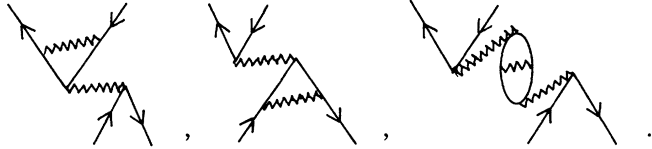


while repeated iterations of the ring kernel alone yields the ring diagrams such as



Cross terms between K_{ladder} and K_{ring} that come from iterations of $K^{\text{RPA(TDA)}}$ give diagrams termed as ring in conjunction with ladder (RCL) diagrams.

Examples of RCL diagrams are of the form



If all of the interaction lines contributed by the ring kernel are deleted in a ring diagram of RCL diagram, the remaining pieces are all ladder diagrams. This allows the RPA (TDA) Bethe-Salpeter equation to be split into two equations (of the standard "two-potential" form)

$$i\Pi^{\text{RPA(TDA)}} = i\Pi^{\text{ladder}} + i\Pi^{\text{ladder}} K_{\text{ring}}^{\text{RPA(TDA)}} i\Pi^{\text{RPA(TDA)}} \quad (2.15)$$

and

$$i\Pi^{\text{ladder}} = i\Pi^{(0)} + i\Pi^{(0)} K_{\text{ladder}}^{\text{RPA(TDA)}} i\Pi^{\text{ladder}}. \quad (2.16)$$

It is possible to show⁵ that Eqs. (2.15) and (2.16) lead to the following set of equations:

$$i\Pi_{\beta\alpha;\gamma\delta}^{\text{RPA(TDA)}}(x,x') = \psi_{\beta}(\mathbf{x})\psi_{\alpha}^*(\mathbf{x})\psi_{\gamma}^*(\mathbf{x}')\psi_{\delta}(\mathbf{x}') \int i\tilde{\Pi}_{\beta\alpha;\gamma\delta}^{\text{RPA(TDA)}}(\omega) e^{-i\omega(x^0-x'^0)} \frac{d\omega}{2\pi}, \quad (2.17)$$

$$i\tilde{\Pi}_{\beta\alpha;\gamma\delta}^{\text{RPA(TDA)}}(\omega) = i\tilde{\Pi}_{\beta\alpha;\gamma\delta}^{\text{ladder RPA(TDA)}}(\omega) + i\tilde{\Pi}_{\beta\alpha;\nu\mu}^{\text{ladder RPA(TDA)}}(\omega) \tilde{K}_{\nu\mu\sigma\rho}^{\text{ring RPA(TDA)}}(\omega) i\tilde{\Pi}_{\sigma\rho;\gamma\delta}^{\text{RPA(TDA)}}(\omega), \quad (2.18)$$

$$i\tilde{\Pi}_{\beta\alpha;\gamma\delta}^{\text{ladder RPA(TDA)}}(\omega) = \int i\Sigma_{\beta\alpha;\gamma\delta}^{\text{RPA(TDA)}}(\omega, a) \frac{da}{4\pi}, \quad (2.19)$$

$$i\Sigma_{\beta\alpha;\gamma\delta}^{\text{RPA(TDA)}}(\omega, a) = i\Sigma_{\beta\alpha;\gamma\delta}^{(0)\text{RPA(TDA)}}(\omega, a) + \int i\Sigma_{\beta\alpha;\nu\mu}^{(0)\text{RPA(TDA)}}(\omega, a) \tilde{K}_{\nu\mu\sigma\rho}^{\text{ladder RPA(TDA)}} \left[\frac{a-v}{2} \right] i\Sigma_{\sigma\rho;\gamma\delta}^{\text{RPA(TDA)}}(\omega, v) \frac{dv}{4\pi}, \quad (2.20)$$

$$i \Sigma_{\beta\alpha; \gamma\delta}^{(0)\text{RPA}}(u, v) = i \bar{\Pi}_{\beta\alpha; \gamma\delta}^{(0)} \left(\frac{1}{2}(u+v), \frac{1}{2}(v-u) \right), \quad (2.21)$$

$$i \Sigma_{\beta\alpha; \gamma\delta}^{(0)\text{TDA}}(u, v) = i \bar{\Pi}_{\beta\alpha; \gamma\delta}^{(0)} \left(\frac{1}{2}(u+v), \frac{1}{2}(v-u) \right) \theta(\beta-F) \theta(F-\alpha), \quad (2.22)$$

where

$$\bar{K}_{\nu\mu\sigma\rho}^{\text{ring RPA(TDA)}}(\omega) = \int e^{i\omega(z^0-z'^0)} \langle \nu\rho | \Delta(z-z') | \mu\sigma \rangle d(z^0-z'^0) \theta_{\text{RPA(TDA)}}^{\nu\mu\sigma\rho}, \quad (2.23a)$$

$$\bar{K}_{\nu\mu\sigma\rho}^{\text{ladder RPA(TDA)}}(\omega) = - \int e^{i\omega(z^0-z'^0)} \langle \nu\rho | \Delta(z-z') | \sigma\mu \rangle d(z^0-z'^0) \theta_{\text{RPA(TDA)}}^{\nu\mu\sigma\rho}, \quad (2.23b)$$

and

$$\bar{\Pi}_{\beta\alpha; \gamma\delta}^{(0)}(w_1, w_2) = \int e^{i\omega_1(y^0-t') + i\omega_2(t'-t)} \Pi^{(0)}(y^0, t; t', t'+) d(y^0-t') d(t'-t). \quad (2.24)$$

We note that, for an instantaneous interaction, one may write

$$\Delta(\mathbf{x} - \mathbf{x}') = -i \delta(x^0 - x'^0) V(\mathbf{x} - \mathbf{x}'). \quad (2.25)$$

Using the instantaneous nucleon-nucleon interaction in the RPA (TDA) integral equations above reduces the integral equations to the conventional matrix equations for the RPA (TDA) admixture coefficients and excitation spectrum.³⁻⁵

The discussion above generalized the RPA (TDA) equations (which yield the nuclear excitation spectrum and particle-hole admixture coefficients) to include retarded nucleon-nucleon interactions. We now summarize standard results that allow one to calculate the nuclear electron-scattering cross sections if the nuclear excitation spectrum and particle-hole admixture coefficient are known. In the one-photon-exchange approximation (linear response) and ignoring nuclear recoil, one has the following equation:⁶

$$\begin{aligned} \frac{d^2\bar{\sigma}(k_i^{\mu} \rightarrow k_f^{\mu})}{d\Omega dE_2} &= 4\pi\sigma_M \left[1 + \frac{2E_1 \sin^2\theta/2}{M_T} \right]^{-1} \delta(\omega - \omega_{\bar{n}}) \\ &\times \left\{ \left[\frac{(\omega^2 - \mathbf{q}\cdot\mathbf{q})^2}{(\mathbf{q}\cdot\mathbf{q})^2} \right] \sum_{J=0}^{\infty} \frac{|\langle f | \hat{M}_J^{\text{Coul}}(q) | i \rangle|^2}{2J_i + 1} \right. \\ &\left. + \left[\tan^2 \frac{\theta}{2} + \frac{\mathbf{q}\cdot\mathbf{q} - \omega^2}{2\mathbf{q}\cdot\mathbf{q}} \right] \sum_{J=1}^{\infty} \left[\frac{|\langle f | \hat{T}_J^{\text{el}}(q) | i \rangle|^2}{2J_i + 1} + \frac{|\langle f | \hat{T}_J^{\text{mag}}(q) | i \rangle|^2}{2J_i + 1} \right] \right\}, \quad (2.26) \end{aligned}$$

where σ_M is the Mott cross section, E_1 is the electron's initial energy, E_2 is the electron's final energy, $\omega = E_1 - E_2$ is the electron energy loss, \mathbf{q} is the momentum transferred to the electron, M_T is the mass of the target nucleus, J_i is the total angular momentum of the initial nuclear state $|i\rangle$, $\omega_{\bar{n}}$ is the excitation energy of the final nuclear state $|f\rangle$ relative to the initial nuclear state, and θ is the electron-scattering angle. The Coulomb multipole operators \hat{M}_J^{Coul} and current multipole operators \hat{T}_J^{el} and \hat{T}_J^{mag} are defined in terms of spherical harmonics $Y_{lm}(\hat{\mathbf{x}})$, vector spherical harmonics $\mathbf{Y}_{JJ_1}^M(\mathbf{x})$, spherical Bessel functions $j_l(x)$, and the nuclear current operator $\hat{j}^{\mu}(\mathbf{x}) \equiv \hat{j}^{\mu}(\mathbf{x}, x^0=0)$ as

$$\hat{M}_{JM}^{\text{Coul}}(q) \equiv \int j_J(q\mathbf{x}) Y_{JM}(\mathbf{x}) \hat{j}^0(\mathbf{x}) d^3\mathbf{x}, \quad (2.27a)$$

$$\hat{T}_{JM}^{\text{el}}(q) \equiv \frac{1}{q} \int \text{curl}[j_J(q\mathbf{x}) \mathbf{Y}_{JJ_1}^M(\hat{\mathbf{x}})] \cdot \hat{\mathbf{j}}(\mathbf{x}) d^3\mathbf{x}. \quad (2.27b)$$

$$\hat{T}_{JM}^{\text{mag}}(q) \equiv \int j_J(q\mathbf{x}) \mathbf{Y}_{JJ_1}^M(\hat{\mathbf{x}}) \cdot \hat{\mathbf{j}}(\mathbf{x}) d^3\mathbf{x}. \quad (2.27c)$$

Summing the cross section over all final states gives

$$\begin{aligned} \frac{d^2\bar{\sigma}}{d\Omega dE_2} &= \sigma_M \left[1 + \frac{2E_1 \sin^2(\theta/2)}{M_T} \right]^{-1} \\ &\times \left[\frac{(\omega^2 - \mathbf{q}\cdot\mathbf{q})^2}{(\mathbf{q}\cdot\mathbf{q})^2} S_L(\mathbf{q}, \omega) \right. \\ &\left. + \left[\frac{\mathbf{q}\cdot\mathbf{q} - \omega^2}{2\mathbf{q}\cdot\mathbf{q}} + \tan^2 \frac{\theta}{2} \right] S_T(\mathbf{q}, \omega) \right], \quad (2.28) \end{aligned}$$

where the longitudinal and transverse structure functions $S_L(\mathbf{q}, \omega)$ and $S_T(\mathbf{q}, \omega)$, respectively, are given by

$$S_L(\mathbf{q}, \omega) = \sum_f \delta(\omega - \omega_f) |\langle \Psi_f | \hat{j}^0(\mathbf{q}) | \Psi_i \rangle|^2, \quad (2.29a)$$

$$S_T(\mathbf{q}, \omega) = \sum_f \delta(\omega - \omega_f) \sum_{\lambda=\pm 1} |\langle \Psi_f | \hat{\mathbf{j}}(\mathbf{q}) \cdot \hat{\mathbf{e}}_{\lambda}(\mathbf{q}) | \Psi_i \rangle|^2, \quad (2.29b)$$

where the $\hat{\mathbf{e}}_{\lambda}(\hat{\mathbf{q}})$ are the components of a unit spherical basis with $\hat{\mathbf{q}} = \hat{\mathbf{e}}_0(\hat{\mathbf{q}})$, and the current density operators $\hat{j}^{\mu}(\mathbf{q})$ are the Fourier transforms of the space-time current operators $\hat{j}^{\mu}(\mathbf{x})$,

$$\int e^{-i\mathbf{q}\cdot\mathbf{x}} \hat{j}^{\mu}(\mathbf{x}) d^3\mathbf{x} = \hat{j}^{\mu}(\mathbf{q}). \quad (2.30)$$

We shall calculate, in a model problem, the longitudinal

response defined as

$$\frac{d\sigma_L}{d\Omega} \equiv \frac{1}{\sigma_M} \left[1 + \frac{2E_1 \sin^2 \theta / 2}{M_T c^2} \right]^{-1} \times \frac{(\omega^2 - \mathbf{q} \cdot \mathbf{q})^2}{(\mathbf{q} \cdot \mathbf{q})^2} S_L(\mathbf{q}, \omega). \quad (2.31)$$

The delta functions including $\omega - \omega_n$ dictate that the cross section will have a nonzero value only when the energy transfer ω is consistent with the nuclear excitation spectrum. Consequently, the excitation spectrum calculated in the TDA or RPA results in a prediction of the peaks of the observed electron-scattering cross section as one varies the energy transferred. While the excitation spectrum determines the peaks in the cross section, the admixture coefficients $C_{\beta\alpha}^{(n)}$ are necessary for the calculation of the reduced matrix elements of the multipole operator which determine the shape of the cross section as one varies the momentum transfer. In order to extract these matrix elements one writes the current density in terms of nuclear Hilbert space fermion creation operators c_α^\dagger and destruction operators c_β as

$$\hat{j}^\mu(\mathbf{x}) = \sum_{\alpha\beta} \psi_\alpha^\dagger(\mathbf{x}) j^\mu(\mathbf{x}) \psi_\beta(\mathbf{x}) c_\alpha^\dagger c_\beta, \quad (2.32)$$

where $\psi_\beta(\mathbf{x})$ is a single-particle wave function corresponding to the state label β . We note $\hat{j}^\mu(x)$ is an operator in the first quantized wave-function space containing, for example, nucleon derivative or spin operators. The nuclear matrix element of \hat{j}^μ is given by

$$\langle f | \hat{j}^\mu(\mathbf{x}) | i \rangle = \sum_{\alpha\beta} \psi_\alpha^\dagger(\mathbf{x}) j^\mu(\mathbf{x}) \psi_\beta(\mathbf{x}) \langle f | c_\alpha^\dagger c_\beta | i \rangle. \quad (2.33)$$

Assuming that the initial state of the nucleus is the ground state, and the final state has energy $\hbar\omega_n$ above the ground state allows

$$\begin{aligned} \langle f | \hat{j}^\mu(\mathbf{q}) | i \rangle &= \int e^{-i\mathbf{q} \cdot \mathbf{x}} \langle f | \hat{j}^\mu(\mathbf{x}) | i \rangle d^3x \\ &= \sum_{\alpha\beta} \int e^{-i\mathbf{q} \cdot \mathbf{x}} \psi_\alpha^\dagger(\mathbf{x}) j^\mu(\mathbf{x}) \psi_\beta(\mathbf{x}) d^3x C_{\alpha\beta}^{(n)*}. \end{aligned} \quad (2.34)$$

In similar fashion, the matrix elements of the multipole operators are given by⁶

$$\langle f | \hat{M}_{JM}^{\text{Coul}}(q) | i \rangle = \sum_{\alpha\beta} \int j_J(qx) Y_{JM}(\hat{\mathbf{x}}) \psi_\alpha^\dagger(\mathbf{x}) j^0(\mathbf{x}) \psi_\beta(\mathbf{x}) d^3x C_{\alpha\beta}^{(n)*}, \quad (2.35a)$$

$$\langle f | \hat{T}_{JM}^{\text{el}}(q) | i \rangle = \frac{1}{q} \sum_{\alpha\beta} \int \psi_\alpha^\dagger(\mathbf{x}) \text{curl}[j_J(qx) \mathbf{Y}_{J1}^M(\hat{\mathbf{x}})] \cdot \mathbf{j}(\mathbf{x}) \psi_\beta(\mathbf{x}) d^3x C_{\alpha\beta}^{(n)*}, \quad (2.35b)$$

$$\langle f | \hat{T}_{JM}^{\text{mag}}(q) | i \rangle = \sum_{\alpha\beta} \int \psi_\alpha^\dagger(\mathbf{x}) j_J(qx) \mathbf{Y}_{J1}^M(\hat{\mathbf{x}}) \cdot \mathbf{j}(\mathbf{x}) \psi_\beta(\mathbf{x}) d^3x C_{\alpha\beta}^{(n)*}. \quad (2.35c)$$

Thus, once a (TDA) RPA calculation yields a nuclear excitation spectrum and the corresponding admixture coefficients, the electron-scattering cross section can be calculated from Eqs. (2.26) and (2.35).

III. A MODEL PROBLEM

In order to study the effects of retardation and apply the formalism developed in the previous section, we now introduce a model Lagrangian. The model is chosen so that, as the velocity of meson propagation approaches infinity, standard instantaneous results are obtained. The model Lagrangian adopted contains a fermion field ψ and a scalar boson field φ and may be written as

$$\mathcal{L} = \mathcal{L}_\psi + \mathcal{L}_\varphi^{(\alpha)} - ig : \psi^\dagger(x) \varphi(x) \psi(x) :, \quad (3.1)$$

where

$$\begin{aligned} \mathcal{L}_\psi &= \frac{i}{2} \psi^\dagger \frac{\partial}{\partial t} \psi - \frac{i}{2} \psi \frac{\partial}{\partial t} \psi^\dagger - \frac{\nabla \psi^\dagger \cdot \nabla \psi}{2M_N} \\ &\quad - \psi^\dagger(x) (-V_0 + \frac{1}{2} M_N \omega_{\text{osc}}^2 \mathbf{x} \cdot \mathbf{x}) \psi(x), \end{aligned} \quad (3.2)$$

and

$$\mathcal{L}_\varphi^{(\alpha)} = \frac{1}{2} \left[\left[\alpha \frac{\partial \varphi}{\partial t} \right]^2 - \nabla \varphi \cdot \nabla \varphi - m_\varphi^2 \varphi^2 \right]. \quad (3.3)$$

For this Lagrangian the field equations for ψ and φ are

$$i \frac{\partial \psi}{\partial t} = - \frac{\nabla^2 \psi}{2M_N} + (-V_0 + \frac{1}{2} M_N \omega_{\text{osc}}^2 \mathbf{x}^2) \psi(x) + ig \varphi(x) \psi(x), \quad (3.4a)$$

$$\alpha^2 \frac{\partial^2}{\partial t^2} \varphi - \nabla^2 \varphi + m_\varphi^2 \varphi = -ig : \psi^\dagger(x) \psi(x) :. \quad (3.4b)$$

The meson field propagator $\Delta_F^{(\alpha)}(x-x')$ for the $\mathcal{L}_\varphi^{(\alpha)}$ piece of the Lagrangian [Eq. (3.3)] is given by

$$i \Delta_F^{(\alpha)}(x-x') \equiv i \int \frac{e^{-ik^\mu(x-x')_\mu}}{(\alpha k^0)^2 - \mathbf{k}^2 - m_\varphi^2 + i\epsilon} \frac{d^4k}{(2\pi)^4}. \quad (3.5)$$

The meson propagator $\Delta_F^{(\alpha)}$ contains a parameter (α) which is used to switch off and on retardation in the fermion-boson system. When $\alpha=1$, the scalar meson propagates at finite speeds, while $\alpha=0$ yields the instantaneous meson propagator whose space-time Fourier transform contains a delta function in $x^0 - x'^0$ times a Yukawa expression in $|\mathbf{x} - \mathbf{x}'|$.

In order to make the connection with standard instantaneous results, we adopt values for the meson mass m_φ and the coupling constant g that lead to a conventional Yukawa phenomenological $N-N$ potential.⁷

The model nucleon Lagrangian \mathcal{L}_ψ is neither Lorentz

invariant nor translationally invariant. By not using the Dirac Lagrangian, problems with the negative-energy nucleon state are avoided. One could, of course, use a Dirac form and simply suppress the negative-energy states. We note the primary interest here is to investigate the effect of using retarded interactions on previous nonrelativistic calculations of nuclear structure.

The assumed harmonic-oscillator potential in \mathcal{L}_ψ , which breaks translational invariance, admits a discrete spectrum to the noninteracting part of the Hamiltonian, thus permitting the construction of a localized N -nucleon noninteracting ground state. Furthermore, the harmonic-oscillator wave functions and propagators have a convenient closed form. In principle, the oscillator could be deleted and Hartree states used to create the finite nucleus ground state and propagators but the harmonic-oscillator basis is sufficient for the present model investigation (and has been used often in previous particle-hole calculations).

The interaction Lagrangian is normal ordered with respect to the ground state of the noninteracting Hamiltonian to more precisely define the model problem. The normal ordering removes ambiguities resulting from the fact that the ψ fields are operators and the order in which they appear is important.

IV. RESULTS

Using the formalism outlined in Sec. II and the simple model Lagrangian discussed in Sec. III, we have performed TDA calculations for low-lying ($\sim 1\hbar\omega_{\text{osc}}$) particle-hole states in the mass-16 system. The particle-hole space was truncated to include $2s(1p)^{-1}$ and $1d(1p)^{-1}$ states. Thus, the states considered would naturally arise in a study of ^{16}O low-lying particle-hole states in a calculation where spin and isospin degrees of freedom were suppressed. The inclusion of these discrete symmetries (spin, isospin) could easily be included in the model problem but should not be important for determining the energy dependence and magnitude of the retardation correction. The particle-hole states considered can couple to angular momentum $L = 1, 2$, or 3 .⁸

The form of the scalar meson propagator, $[(q_0^2 - m^2) - q^{-2} + i\epsilon]^{-1}$, suggests that differences between a single finite velocity meson exchange and the associated instantaneous Yukawa potential (same couplings and meson mass range, but $q_0 \equiv 0$) should be small when $(q^0/m) \ll 1$. Since both the RPA TDA involve multiple meson-exchange diagrams with an associated integration over all internal meson energies, the possibility exists for a non-negligible difference between the nuclear structure calculated for a retarded meson-exchange nucleon-nucleon interaction and that for an instantaneous Yukawa nucleon-nucleon potential. In any event, it is useful to make quantitative estimates of the difference. In the multiple-meson-exchange diagrams, the contribution of the nucleon propagators to the integrand is diminished as the nucleon energy moves away from the particle or hole energies. Energy conservation at the meson-nucleon vertices, along with this behavior of the nucleon propagator, suggests that retardation effects may begin to manifest

themselves when the particle-hole energies are on the order of the meson mass. In order to test this conjecture and the extent to which retardation affects traditional nuclear structure predictions, we have performed TDA calculations of the excitation spectrum, admixture coefficients (residues of the polarization propagator), and the nuclear longitudinal linear response for various magnitudes of the unperturbed particle-hole energies.

Before discussing the excitation spectrum obtained from a solution of the coupled integral equations given by Eqs. (2.17)–(2.20) in the TDA and the model problem defined above, it is useful to study the TDA ring and ladder kernels defined by Eqs. (2.23a) and (2.23b), respectively. The ring and ladder kernels (interactions) are shown as a function of energy ω in Figs. 1(a)–1(f) for the diagonal $1d(1p)^{-1}$, $J=1, 2, 3$ matrix elements. Note that, with the conventions we adopt, one expects both the TDA ring and ladder kernels to be pure imaginary for an instantaneous real interaction $V(\mathbf{x} - \mathbf{x}')$. When ω is less than the meson mass, the kernels remain pure imaginary for retarded interactions associated with meson exchange. However, as is shown in Figs. 1(a)–1(f), both the ring and ladder kernels obtain a real part (loss of Hermiticity) when $\omega \gtrsim m_{\text{meson}}$ and therefore real meson production is possible. Such diagrams are not included in our model and thus the effect is to have an interaction with a real and imaginary part (much like a complex optical potential that allows flux to be lost above the threshold for reaction channels not included in the model space). For an instantaneous interaction the meson degree of freedom is completely suppressed and the effects associated with real meson production do not appear at any ω . We note from the figures that, for $J=2$ and 3 , the variation of the ladder kernel with ω is greater than the ω variation of the ring kernel. The vanishing of the ring kernel for $J=2$ in the model space studied [see Figs. 1(c) and (d)] is due to a cancellation between Moshinsky brackets and is independent of the interaction adopted.

As the energy ω of the exchanged meson goes to ∞ , we find that the kernels damp to zero. However, in the range of ω shown in the figures (for $\omega > m$), oscillatory and other transient behavior is superimposed on the damping limit that occurs for very large ω . It is not surprising that the kernels are damped at large ω . This occurs because, in a given nuclear shell model, the two interacting nucleons have a fixed average separation $x - x'$. For large ω the typical meson exchange intergrand contained in

$$\tilde{K}(\omega) = \int e^{i\omega\tau} \langle \Delta(\tau, \mathbf{x} - \mathbf{x}') \rangle d\tau$$

becomes rapidly oscillating as τ varies and satisfies $\omega\tau > 1$. Therefore, contributions to $\tilde{K}(\omega)$ from meson emission and absorption processes separated in time by more than $1/\omega$ are suppressed. Thus, the time separation of such effective processes decreases as the exchanged meson becomes more energetic. The range R of effective meson mediated nucleon-nucleon interactions must therefore satisfy

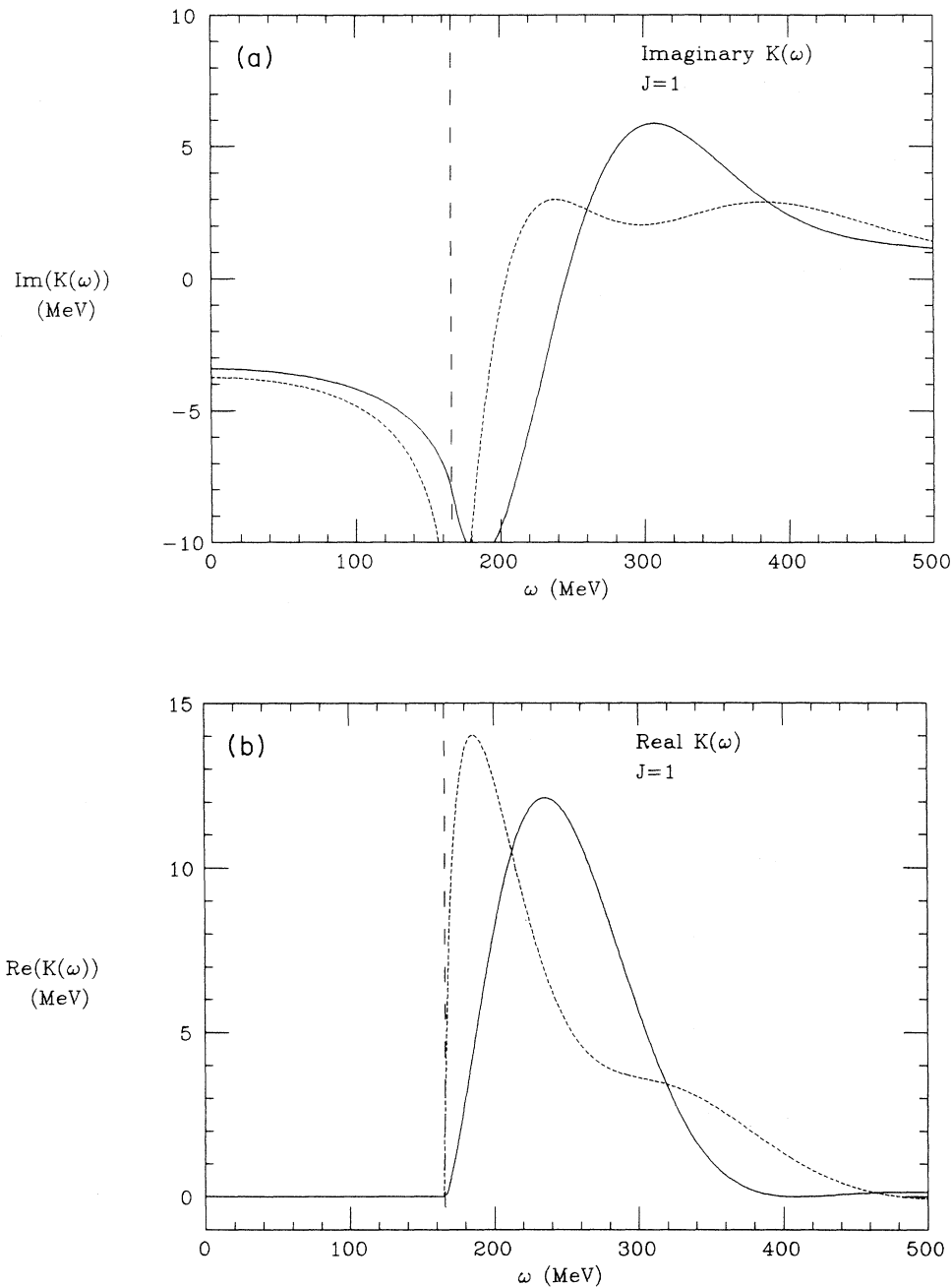


FIG. 1. The $1d(1p)^{-1}$ diagonal ring kernels (solid line) and ladder kernels (thin-dashed line) defined by Eqs. (2.23a) and (2.23b), respectively, as a function of ω , the energy of the exchanged meson. Real and imaginary parts of $\bar{K}(\omega)$ are shown separately for $J=1,2,3$ as indicated. The wide-dashed vertical line indicates $\omega=m$, where m is the mass of the exchanged meson. For an instantaneous interaction one obtains a pure imaginary $\bar{K}(\omega)$ that is independent of ω .

$$R \approx \tau \leq \frac{1}{\omega}.$$

As ω increases, eventually $\overline{x-x'} > R$ and the kernel damps (because, on the average, the nucleons are not close enough for the increasingly short-range interaction to be effective). Note that the different ω dependence of

the ring and ladder integrals makes it unwise, without further study, to drop the ladder contributions and simply renormalize the ring kernel.

A summary of the results for the $J=1$ and 3 excitation spectra as a function of unperturbed particle-hole energies for both retarded and instantaneous nucleon-nucleon interactions is given in Figs. 2 and 3. In each figure one

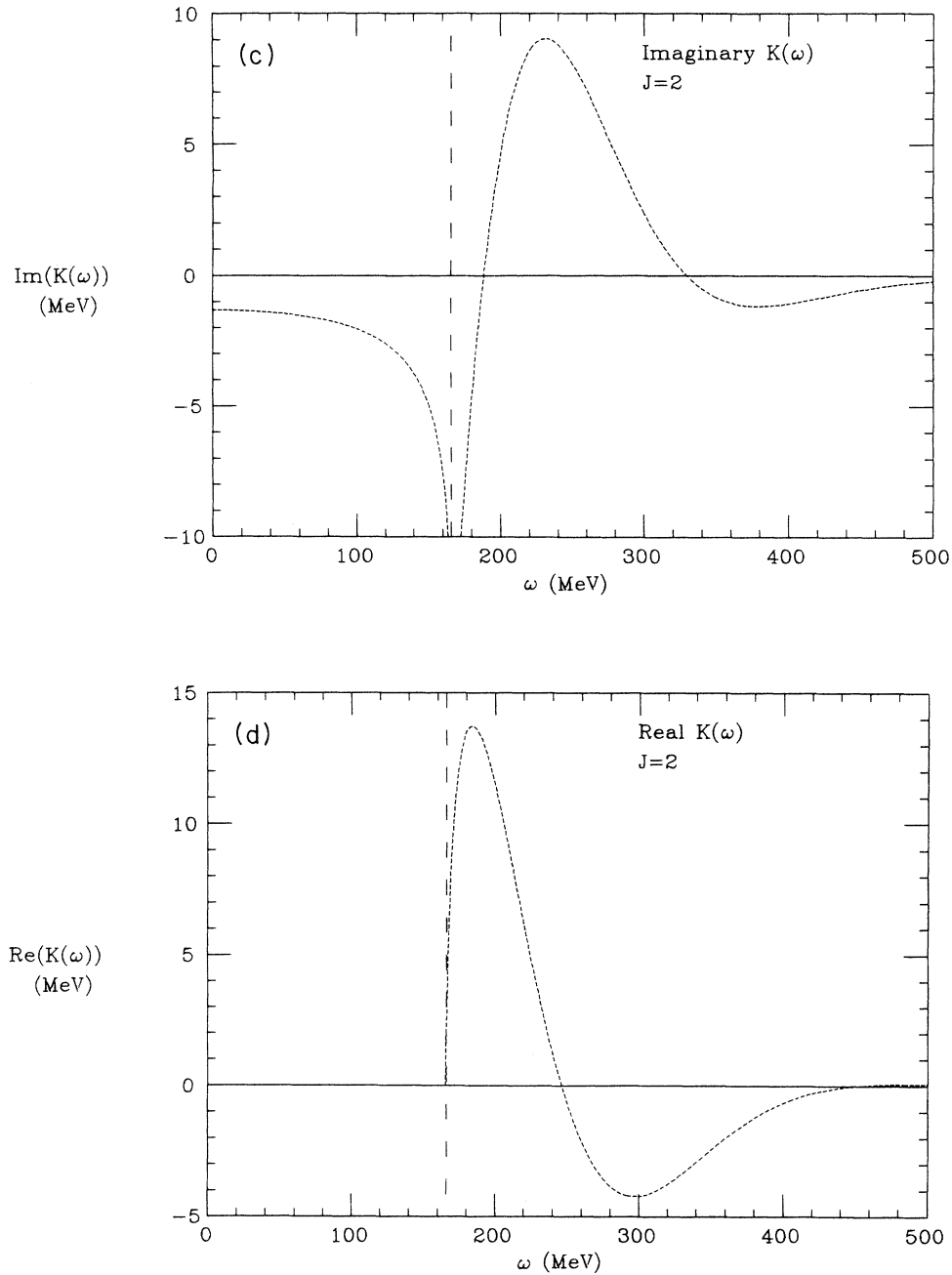


FIG. 1. (Continued).

finds that the retarded calculation prediction for $E - E_{p-h}$ differs from the instantaneous prediction by less than 10% when the particle-hole energies are less than approximately half the meson mass. As the particle-hole energies become greater than $m/2$, the excitation spectrum for the retarded interaction changes from the instantaneous interaction spectrum for the $J=1$ and 3 cases. (As noted earlier, the $J=2$ ring kernel vanishes identically for the model under consideration. This results in a prediction for the $J=2$ energy state which is essentially independent of whether a retarded or instan-

aneous interaction is used and therefore this case is not shown.) Using a retarded interaction, the splitting between the two $J=1$ states, as shown by Fig. 3, is about 2.5 times that calculated for the instantaneous interaction for particle-hole energies in the vicinity of the exchanged mass.

Figures 4(a)–(c) show how the residues of the upper energy $J=1$ state polarization propagators vary with particle-hole energy for both the scalar meson nucleon-nucleon interaction and its instantaneous reduction. The residue of the polarization propagator that is diagonal in the

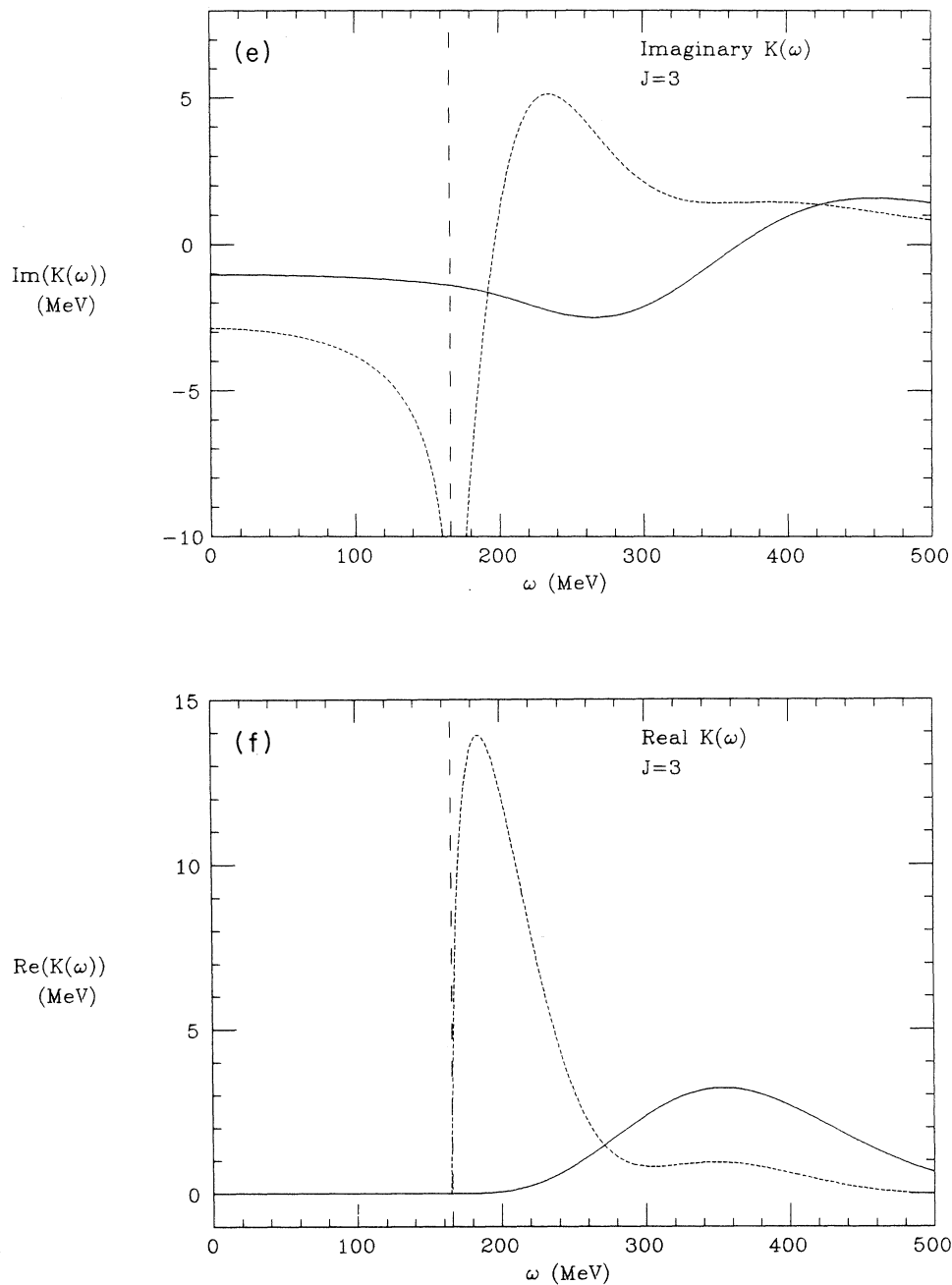


FIG. 1. (Continued).

particle-hole labels is the absolute square of the admixture coefficient associated with a given state for that particle-hole configuration [see Eq. (2.7)]. For off-diagonal elements of the polarization propagator, the residue gives the relative phase of the admixture coefficients corresponding to the particle-hole labels of the polarization propagator. In this truncated particle-hole basis there is only one $J=2$ and 3 state that arises from the coupling of the $1d(1p)^{-1}$ particle-hole configuration, so the normalized admixture coefficients for the $J=2$ and 3 states are simply 1 for every particle-

hole energy and thus are not shown.

Figures 4(a)–(c) show that the residue of the polarization propagator for the retarded interaction differs only slightly from the residue for the instantaneous interaction in the region of particle-hole energies studied. Thus, quantities that depend on the coherent sum of absolute squares of admixture coefficients are fairly insensitive to retardation effects. Moreover, even quantities sensitive to off-diagonal products of admixture coefficients in this model should be only negligibly altered by retardation effects when particle-hole energies are less than 80% of

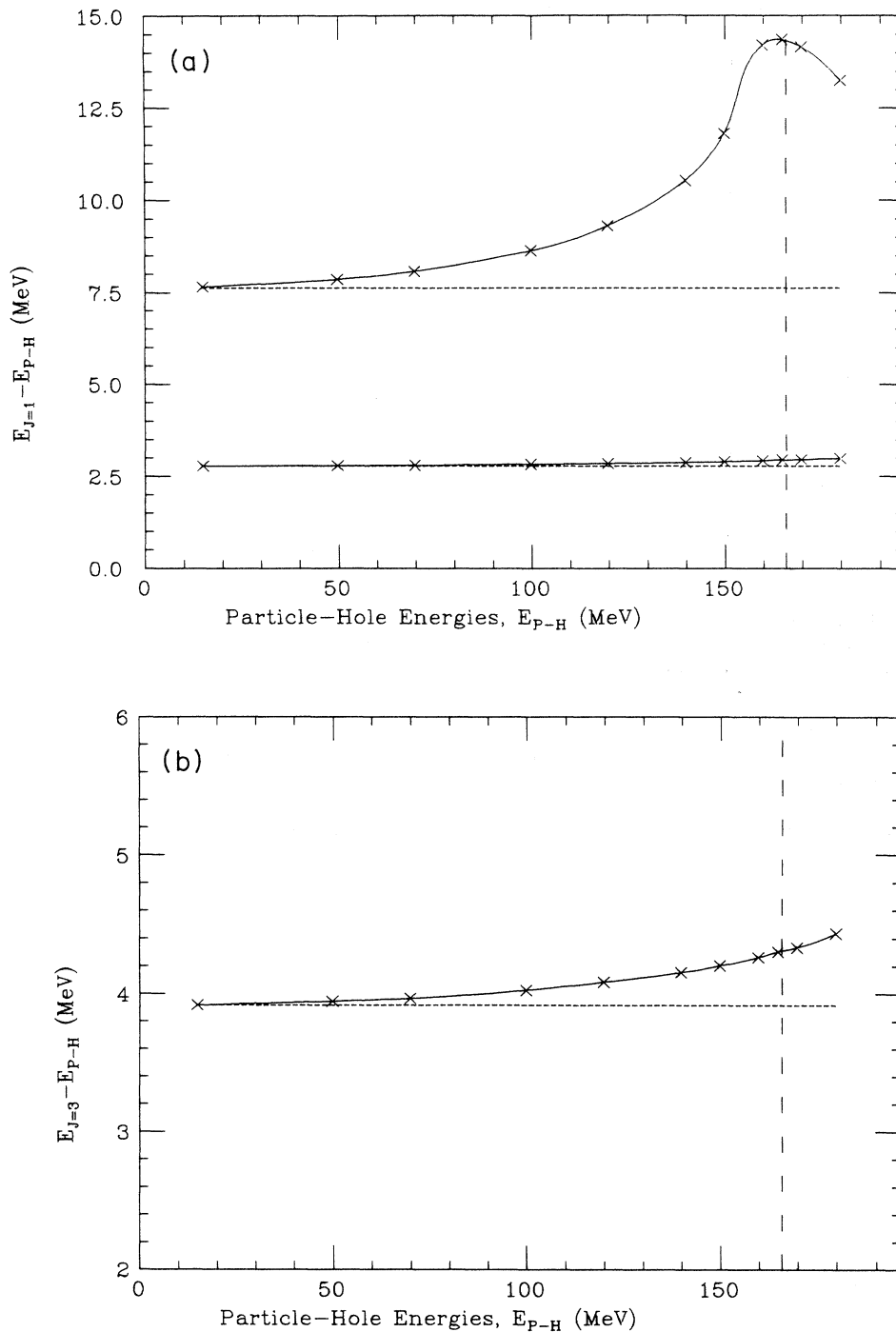


FIG. 2. (a) Comparison of the two $J=1$ excitation energy predictions for particle-hole ($p-h$) states as a function of the unperturbed $p-h$ energies (E_{p-h}). The solid (thin-dashed) lines result from a calculation using a retarded (instantaneous) nucleon-nucleon interaction. The vertical wide-dashed line indicates the energy where $E_{p-h} = m$ (the exchanged meson mass). (b) Same as (a) except the single $J=3$ particle-hole state comparison is shown.

the meson mass.

If the admixture coefficients and excitation spectrum are known, the calculation of the linear response cross section for electron scattering is straightforward using

the equations summarized in Sec. II. The component of the electron-scattering cross section that depends on the Coulomb multipole $\hat{M}_J^{\text{Coul}}(q)$, divided by the Mott cross section, is designated the longitudinal response and

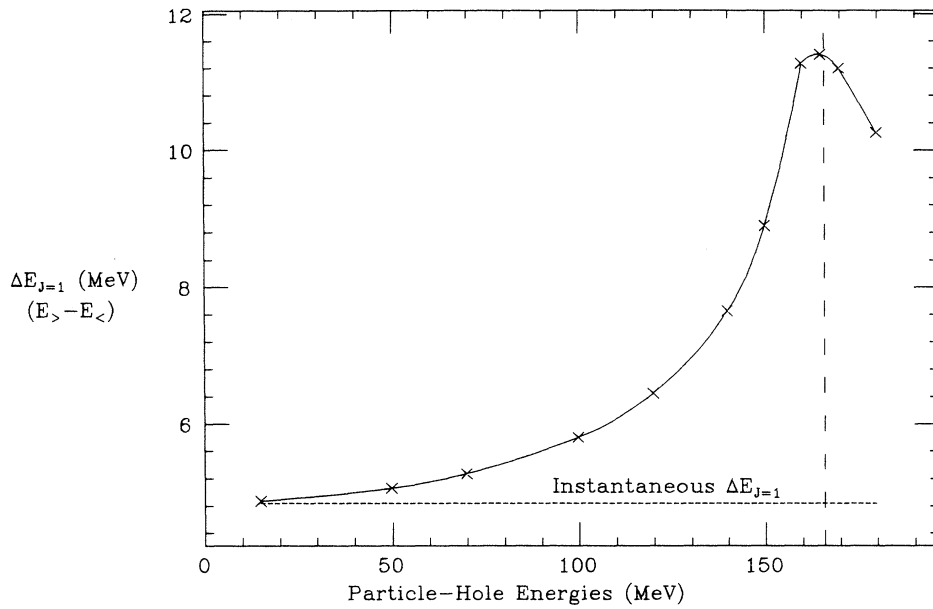


FIG. 3. Energy splitting of the two configuration admixed $J=1$ particle-hole states shown in Fig. 2(a) as a function of the pure particle-hole energies. The $2s$ and $1d$ single-particle energies are assumed degenerate in the model studied. The solid (dashed) line results from using a retarded (instantaneous) interaction.

shown in Figs. 5(a)–(c). The peaks in the longitudinal response, as the energy transferred to the nucleus ω is varied, correspond to the excitation energies of excited nuclear states. The shape of the longitudinal response as

one varies the momentum transfer q while keeping the energy transferred to the nucleus fixed is governed by the admixture coefficients for a given set of orbitals. Figure 5 shows the longitudinal response in the truncated

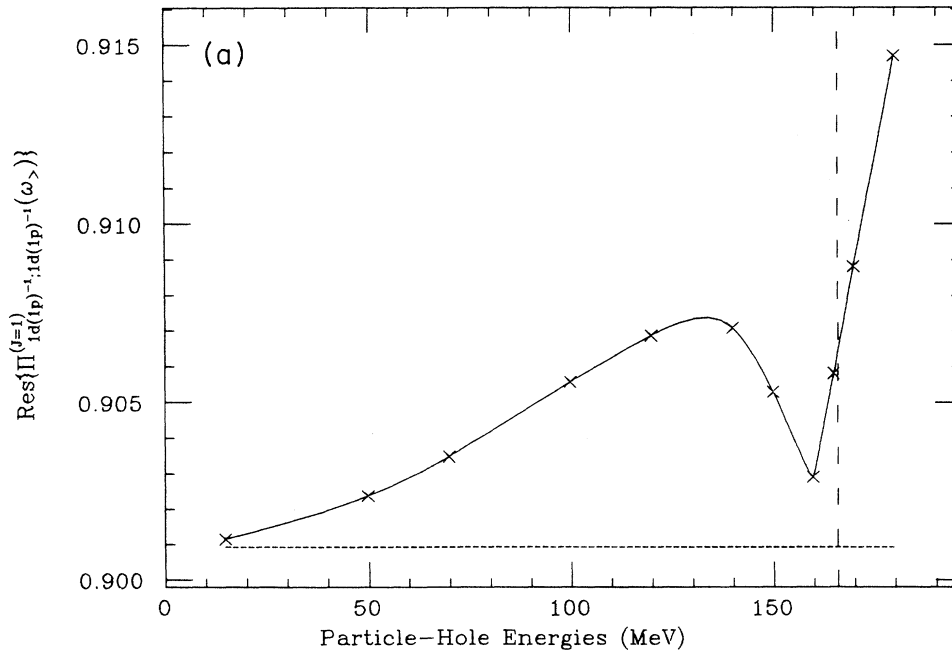


FIG. 4. Residues of the upper energy $J=1$ state polarization propagators as a function of unperturbed particle-hole energy. The solid (dashed) line is for the retarded (instantaneous) interaction. See Eq. (2.7) for the relationship between the residue and pure particle-hole admixture coefficient.

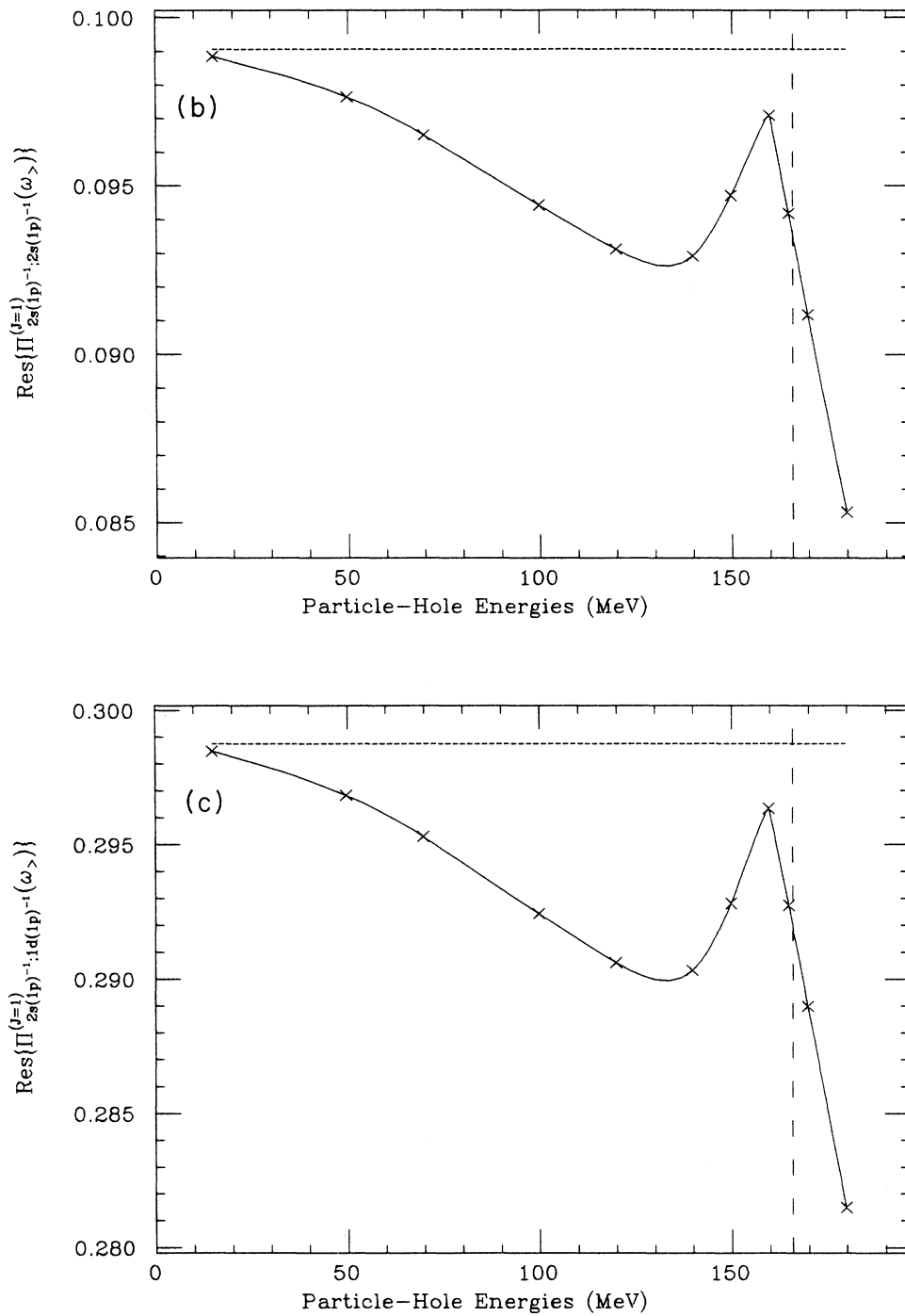


FIG. 4. (Continued).

particle-hole basis at various particle-hole energies with both instantaneous and retarded nucleon-nucleon interactions. The higher energy $J=1$ responses in the figures have been diminished by a factor of 10. Figure 5 shows that, for typical particle-hole energies (~ 15 MeV), the $J=1$ response of a nucleus whose nucleons interact via a

finite velocity scalar meson exchange is virtually identical to that of a nucleus whose nucleons interact via the instantaneous limit of a scalar meson exchange (in the model problem under consideration). As the particle-hole energy increases, the retarded response separates from the instantaneous response. In general, the shape of the

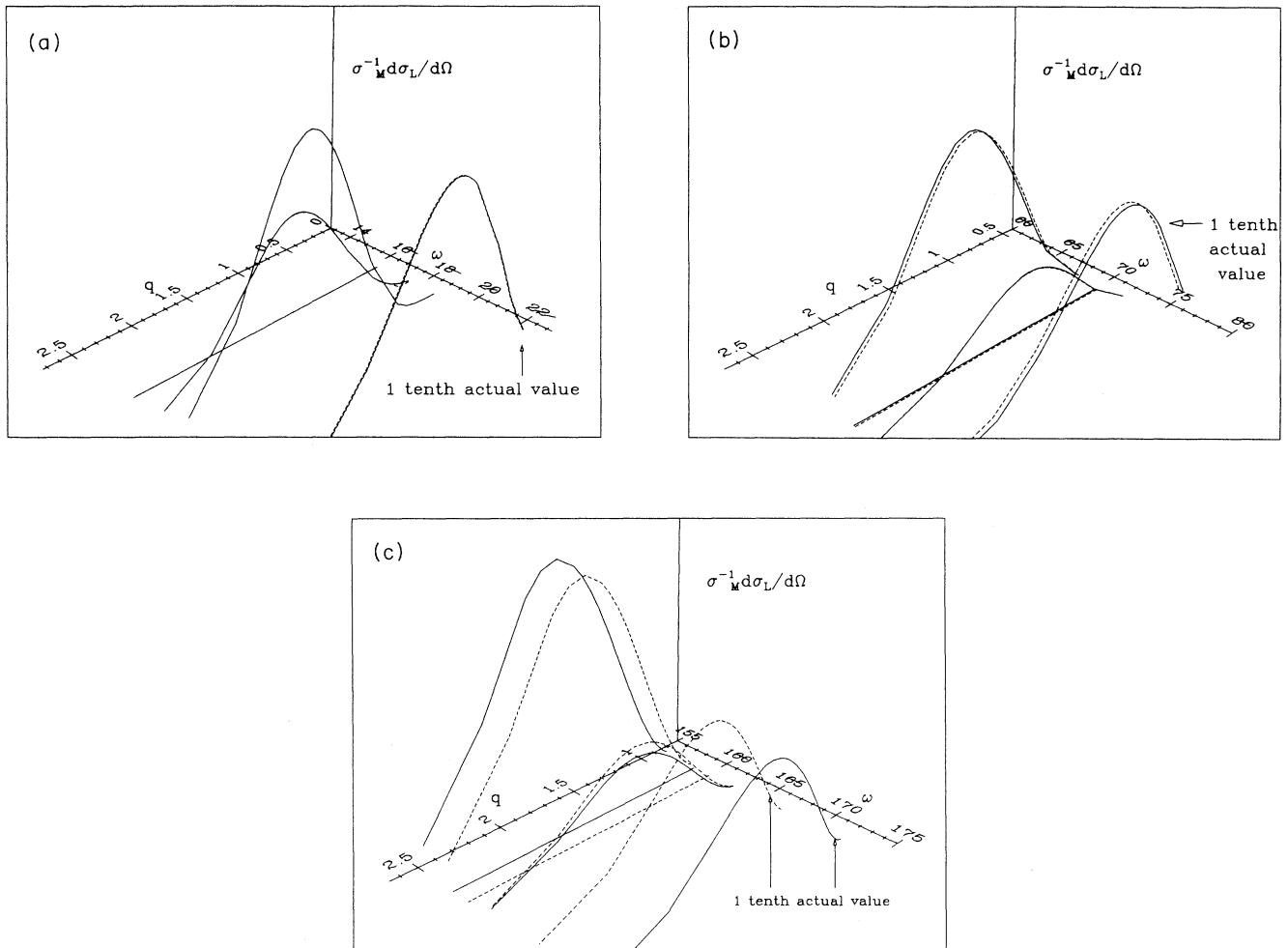


FIG. 5. The longitudinal response defined by Eq. (2.31) plotted as a function of the nuclear excitation energy ω and three-momentum transfer q . The solid (dashed) lines result from a model using a retarded (instantaneous) interaction.

response remains the same in the retarded case and instantaneous case. This is a reflection of the fact that the admixture coefficients do not change dramatically from the incorporation of retardation as the particle-hole energy approaches the meson mass. However, as the particle-hole energies approach the meson mass, the instantaneous response separates from the retarded response due to the change in the nuclear excitation spectrum.

The model calculation discussed herein is more difficult to perform than standard calculations using instantaneous interactions. The main complicating feature is the integral equation for iterating the ladder kernel, Eq. (2.20), and obtaining the ladder polarization propagator Eq. (2.19). Thus, it would be useful to find an accurate but simpler way to obtain the ladder polarization propagator for use in retarded interaction calculations. Moreover, because the ladder terms are sometimes deleted (or included by renormalizing the ring kernel) in RPA calculations, it is of interest to determine the major contribu-

tions (ring, ladder) in the predictions for the excitation spectrum.

It was noted earlier that the ladder interaction often shows more variation with energy ω than the ring interaction. However, an important result is that the impact of this variation of the ladder kernel with energy on the nuclear excitation spectrum is decreased by the fact that the ladder polarization propagator is derived from an integral over the ladder kernel. This integration tends to smooth out the variations in the contribution of the ladder kernel to the ladder polarization propagator as one varies the particle-hole energies. In fact, calculations of the nuclear excitation spectrum and admixture coefficients in which only the ladder diagrams are kept show that the nuclear excitation spectrum and admixture coefficients are essentially identical for instantaneous and retarded meson-exchange nucleon-nucleon interactions at all particle-hole energies up to 10% greater than the meson mass. This results because the analytic structure of the integral in Eq. (2.20) is such that for terms that

contribute to the integral, one can effectively replace $\tilde{K}^{\text{ladder}}(\frac{1}{2}(a-v))$ by $\tilde{K}^{\text{ladder}}(0)$. Indeed, the Π^{ladder} resulting from this approximation is only negligibly different from that obtained using the retarded ladder kernel.

The numerical result obtained above may be understood from the following considerations. First we note

[from Eqs. (2.19) and (2.20)]

$$i\Sigma_{\beta\alpha;\gamma\delta}^{(\text{TDA})}(\omega, v) = 4D_{\beta\alpha}D_{\gamma\delta}h_{\beta\alpha}(\omega, v)T_{\beta\alpha;\gamma\delta}(\omega, v) \quad (\text{no sum over } \beta\alpha, \gamma\delta), \quad (4.1)$$

where

$$T_{\beta\alpha;\gamma\delta}(\omega, v) \equiv \delta_{\beta\gamma}\delta_{\alpha\delta}D_{\beta\alpha}D_{\gamma\delta} + \int \tilde{K}_{\beta\alpha\sigma\rho}^{\text{ladder}(\text{TDA})} \left(\frac{a-v}{2} \right) h_{\sigma\rho}(\omega, a) T_{\sigma\rho;\gamma\delta}(\omega, a) \frac{da}{\pi} \quad (\text{no sum over } \beta\alpha; \gamma\delta) \quad (4.2)$$

and where

$$D_{\beta\alpha} = \begin{cases} \theta(\beta-F)\theta(F-\alpha), & \text{TDA} , \\ \theta(\beta-F)\theta(F-\alpha) + \theta(\alpha-F)\theta(F-\beta), & \text{RPA} . \end{cases} \quad (4.3)$$

The explicit form for $h_{\beta\alpha}$ is found from the expression for $\Sigma^0(\omega, v)$. We obtain

$$h_{\beta\alpha}(\omega, v) = \left[\frac{\theta(\alpha-F)}{v - (2\omega_\alpha + \omega) + i\eta} + \frac{\theta(F-\alpha)}{v - 2(\omega_\alpha + \omega) - i\eta} \right] \left[\frac{\theta(\beta-F)}{v - (2\omega_\beta - \omega) + i\eta} + \frac{\theta(F-\beta)}{v - (2\omega_\beta - \omega) - i\eta} \right]. \quad (4.4)$$

Equation (2.19) now becomes

$$i\Pi_{\beta\alpha;\gamma\delta}^{\text{ladder}(\text{TDA})}(\omega) = \int h_{\beta\alpha}(\omega, v) T_{\beta\alpha;\gamma\delta}(\omega, v) \frac{dv}{\pi} \quad (\text{no sum over } \beta\alpha). \quad (4.5)$$

Assuming that $T_{\beta\alpha;\gamma\delta}(\omega, v)$ has no poles close to the real axis, and given the form of $h_{\beta\alpha}(\omega, v)$, one can conjecture that the major contribution to the ladder polarization propagator comes from those values of $T(\omega, v)$, where v is in the neighborhood of the poles of $h(\omega, v)$, i.e., when

$$v = 2\omega_\alpha + \omega$$

or

$$v = 2\omega_\beta - \omega .$$

In the integral equation for $T(\omega, v)$, the singular nature of $h(\omega, a)$ enhances the contribution of the ladder kernel when

$$a = 2\omega_\rho + \omega$$

or

$$a = 2\omega_\sigma - \omega .$$

Thus, the values of the ladder kernel $\tilde{K}^{\text{ladder}}(x)$ that have the major role in the calculation of the ladder polarization propagator occur when the kernel's argument x has the values

$$x = \frac{a-v}{2} \begin{cases} \omega_\rho - \omega_\alpha , \\ \omega_\rho - \omega_\beta - \omega , \\ \omega_\sigma - \omega_\alpha - \omega , \\ \omega_\sigma - \omega_\beta , \end{cases} \quad (4.6)$$

[note $\tilde{K}^{\text{ladder}}(x) = \tilde{K}^{\text{ladder}}(-x)$]. We are interested in en-

ergies ω that are on the order of the particle-hole energies (to within ~ 10 MeV). That is,

$$\omega \sim \omega_\beta - \omega_\alpha ,$$

where

$$\beta > F < , \quad \alpha < F .$$

In the following we specialize in the TDA model adopted herein. The TDA ladder kernel (2.23b) restricts the state labels (β, σ) to particle state labels and (α, ρ) to hole state labels so that

$$\beta, \sigma > F$$

and

$$\alpha, \rho < F .$$

Consequently, for the truncated Hilbert spaces kept in traditional nuclear structure TDA calculations, the values of the argument of the TDA ladder kernel that enter most prominently in the calculation of the ladder polarization propagator [see Eq. (4.6)], are $\lesssim 30$ MeV. In fact, from Figs. 1(a)-(f), one can see that, for $x \lesssim 30$ MeV, the value of the ladder kernel is essentially the same as $\tilde{K}^{\text{ladder}}(0)$. Thus, it is to be expected that the ladder polarization propagator in the TDA [for the energy region of interest (roughly that of the particle-hole energy)] is very nearly the same whether retarded or instantaneous residual particle-hole interactions are used. Our TDA numerical results for the ladder polarization propagator (for $\omega \sim \omega_{p-h}$) are essentially identical whether a retarded or instantaneous residual interaction is adopted. This conclusion holds for conventional particle-hole energies ($\omega_{p-h} \lesssim 30$ MeV) as well as particle-hole energies up to the order of the meson mass.

The result discussed above allows a great simplification

as can be seen by combining Eqs. (2.19) and (2.20) and using

$$\tilde{K}^{\text{ladder}} = \tilde{K}^{\text{ladder}}(0) .$$

This allows (suppressing subscripts)

$$\begin{aligned} i\tilde{\Pi}^L(\omega) &= \int i\Sigma(\omega, a) \frac{da}{4\pi} \\ &= \int i\Sigma^{(0)}(\omega, a) \frac{da}{4\pi} \\ &\quad + \int \int \frac{da}{4\pi} \frac{dv}{4\pi} i\Sigma^{(0)}(\omega, a) \tilde{K}^{\text{ladder}}(0) i\Sigma(\omega, v) \end{aligned} \quad (4.7)$$

$$= i\Pi^0(\omega) + i\Pi^0(\omega) \tilde{K}^{\text{ladder}}(0) i\tilde{\Pi}^L(\omega) , \quad (4.8)$$

which reduces the integral equation to the familiar algebraic equation that would be present for an instantaneous interaction. This results in a simple form for the ladder polarization propagator which is then to be inserted in the ring kernel algebraic equation (2.18). This allows the set of equation (2.18)–(2.20) to be written in the form of an algebraic equation with a modified kernel

$$K = \tilde{K}^{\text{ladder}}(0) + \tilde{K}^{\text{ring}}(\omega) .$$

We find that use of this approximation, in the model problem considered, results in predictions that are essentially identical to those obtained using the full retarded ladder kernel in the region $\epsilon_{p-h} \leq m_{\text{meson}}$.

We note that the results we have obtained imply that one *cannot* ignore the ladder kernel and that it is important to conclude retardation effects in the ring kernel. We have also found that the effects of retardation can be suppressed in the ladder kernel appearing in the associated ladder polarization propagator integral equation. This reduces the ladder integral equation to a much simpler algebraic equation.

V. CONCLUSIONS AND DISCUSSION

Using many-body techniques, we have developed a set of coupled equations that allow the practical inclusion of

finite velocity intermediate mesons in the nucleon-nucleon interaction adopted for studies of the nuclear linear response in the RPA of TDA. The principal equations involved [(2.18)–(2.20)] first require the solution of an integral equation (2.20) involving the ladder kernel. This provides input into an *algebraic* equation (2.18) involving the ring kernel. A model problem, using a retarded interaction with strength and range similar to standard instantaneous interactions, was studied using the coupled equations discussed above. It was found that the difference (instantaneous versus retarded) between predicted energy-level spectra and form factors was negligible until the particle-hole energies involved were on the order of the mass of the meson exchanged between nucleons in the model. The differences obtained suggest that retardation will not be important for standard low-excitation nuclear structure studies. The predicted nuclear response for isobar particle-nucleon-hole states may be appreciably affected by the introduction of retardation interactions and we intend to investigate this possibility in a model problem.

The fact that the solution of the integral equation (2.20) is integrated over one of the energy variables in Eq. (2.19) [and another in (2.20)] results in the fact that, although

$$\tilde{K}^{\text{ladder}}(E = \frac{1}{2}(v - a))$$

can be strongly dependent on E , nevertheless, the $\tilde{\Pi}^{\text{ladder}}(\omega)$ obtained using $\tilde{K}^{\text{ladder}}(E=0)$ is nearly identical to that obtained using the retarded $\tilde{K}^{\text{ladder}}$. As discussed in the preceding section, this reduces a set of coupled integral equations to a much simpler algebraic matrix equation. While this result was obtained in a particular model problem with a specific choice of retarded interaction, since the analytic structure of the assumed interaction is typical of more realistic N - N interactions, the approximation may be generally useful. Because of the usefulness of the approximation, further investigation of the domain of validity seems warranted.

This work was supported by the National Science Foundation.

¹B. D. Serot, S. E. Koonin, and J. W. Negele, *Phys. Rev. C* **28**, 1679 (1983).

²There have been numerous RPA or TDA relativistic studies, including R. J. Furnstahl, *Phys. Lett.* **152B**, 313 (1985); Michael W. Price and G. E. Walker, *Phys. Rev. C* **38**, 2850 (1988); J. R. Shepard, E. Rost, and J. A. Neil, *ibid.* **40**, 2320 (1989); and John F. Dawson and R. J. Furnstahl, *ibid.* **42**, 2009 (1990). The ring diagrams in these studies can be straightforwardly included without neglecting retardation. The new feature of the present study is to allow for retardation effects in the ladder diagrams as well.

³A. L. Fetter and J. D. Walecka, *Quantum Theory of Many Particle Systems* (McGraw-Hill, New York, 1971), Sec. 60.

⁴D. J. Thouless, *Rep. Prog. Phys.* **27**, 53 (1964); W. Czyz, *Acta Phys. Polon.* **20**, 737 (1961); G. E. Brown, *Many-Body Prob-*

lems (North-Holland, Amsterdam, 1972), Chap. 4.

⁵M. A. Crecca, Ph.D. dissertation, Indiana University 1989. Available from the present authors on request.

⁶T. deForest and J. D. Walecka, *Adv. Phys.* **15**, 1 (1966).

⁷We use $V_0 = 46$ MeV, $m^{-1} = 1.19$ fm, where $g^2 = -4\pi c V_0 (\hbar m)^{-1}$. G. E. Brown and A. D. Jackson, *The Nucleon-Nucleon Interaction* (North-Holland, Amsterdam, 1976), p. 17.

⁸The detailed formulas for the application including the necessary, but cumbersome explicit angular-momentum geometrical coefficients are included in Ref. 5 and is available from the authors on request. The details of the computer codes used to solve the associated integral equation are also discussed in this reference.